Energy 35 (2010) 1447–1454

Contents lists available at ScienceDirect

Energy

journal homepage: www.elsevier.com/locate/energy

A mathematic model of thermoelectric module with applications on waste heat recovery from automobile engine

Y.Y. Hsiao [a,1], W.C. Chang [b,*], S.L. Chen [a,1]

[a] Department of Mechanical Engineering, National Taiwan University, No. 1, Sec. 4, Roosevelt Road, Taipei 106, Taiwan
[b] Department of Mechanical Engineering, Southern Taiwan University, 1, Nantai Street, Yungkang City, Tainan County 710, Taiwan

ARTICLE INFO

Article history:
Received 26 April 2009
Received in revised form
25 November 2009
Accepted 26 November 2009
Available online 23 December 2009

Keywords:
Thermoelectric generator
Thermal resistance
Waste heat
Modeling

ABSTRACT

Over two-thirds energy of fuel consumed by an automobile is discharged to the surroundings as waste heat. The fuel usage can be more efficient if thermoelectric generators (TEG) are used to convert heat energy into electricity. In this study, a thermoelectric module composed of thermoelectric generators and a cooling system is developed to improve the efficiency of an IC engine. Two potential positions on an automobile are chosen to apply this module, e.g. exhaust pipe and radiator to examine the feasibility. To predict the behaviors of this module, a one dimensional thermal resistance model is also build, and the results are verified with experiments.

The maximum power produced from the module is 51.13 $mWcm^{-2}$ at 290 °C temperature difference. The model results show that, TE module presents better performance on the exhaust pipe than on the radiator.

1. Introduction

According to the Otto cycle, during the operating process, it is necessary for internal combustion engine to discharge heat to the atmosphere for completing the thermodynamic process. Consequently, only about 30% energy released from consumed fuel is converted as propelling force, the other 70% is either discharged by exhaust gas, or expelled by the cooling system. Energy lost from dispersed heat can be recovered by several ways, thermoelectric generator (TEG) is considered useful by several auto makers. Through the effect of temperature difference, waste heat can be converted to electricity from the exhaust pipe and radiator on an automobile.

In 1988, Birholz et al. [1] presented the first TEG's application on the automobile. In this research, a single TEG unit using $FeSi_2$ as material was adopted to produce 1 W electric power. Bass et al. [2–6] applied an array with 72 pieces of TEG on a diesel truck. By maintaining 230 °C and 30 °C at hot and cold sides of TEGs respectively, energy conversion efficiency of 4.5% was achieved. Kobayashi et al. [7] used the same amount of SiGe TEGs on a 3000 c.c. petrol engine vehicle. A rectangular section of exhaust pipe was used as the hot source and attached by one side of TEG. On the other side of TEG, a water cooling system was used as a heat sink. At 60 km/h vehicle speed, the exhaust temperature was 1141 °C, and the temperature difference on TEG was 563 °C. The maximum power generated from a single TEG was 1.2 W at 0.7 V with 0.9% thermal efficiency. Ikoma et al. [8] applied HZ-14s (Bi_2Te_3) on a petrol engine vehicle. The maximum power output from TEGs, at vehicle speed of 60 km/h, was 193 W with 2.9% conversion efficiency. Thacher et al. [9] attached HZ-20s (Bi_2Te_3) to a light truck engine. The experimental results showed the power output from TEGs increased with engine speed, and the whole system can produce up to 330 W power.

Matsubara [10,11] used two materials, $YbFe_3CoSb_{12}$ and $YbFe_{3.6}Ni_{0.4}Sb_{12}$, to develop a new TEG. 16 of them were stacked on the exhaust pipe of a 2.0 L passenger car. A maximum power output of 266 W was gained under 475 °C temperature difference condition. Recently, Champier and co-workers [12] applied TE modules on biomass cook stoves to generate electricity to power the fan and light. This commercial TEG is made of Bismuth Telluride, the same material used in this work.

Many experiments have been done to apply TEGs on an automobile, however, only a few works simulated the behaviors of TEG and TE module. The presented model helps to understand the characteristics of TEG, and the effects of engine speed and coolant temperature of radiator on the TE module.

* Corresponding author. Tel.: +886 932815246; fax: + 886 6 2425092.
E-mail addresses: steven919@gmail.com (Y.Y. Hsiao), wcchang@mail.stut.edu.tw (W.C. Chang). slchen01@ccms.ntu.edu.tw (S.L. Chen).
[1] Tel.: +886 2 33662726; fax: +886 2 23631755.

0360-5442/$ – see front matter © 2009 Elsevier Ltd. All rights reserved.
doi:10.1016/j.energy.2009.11.030

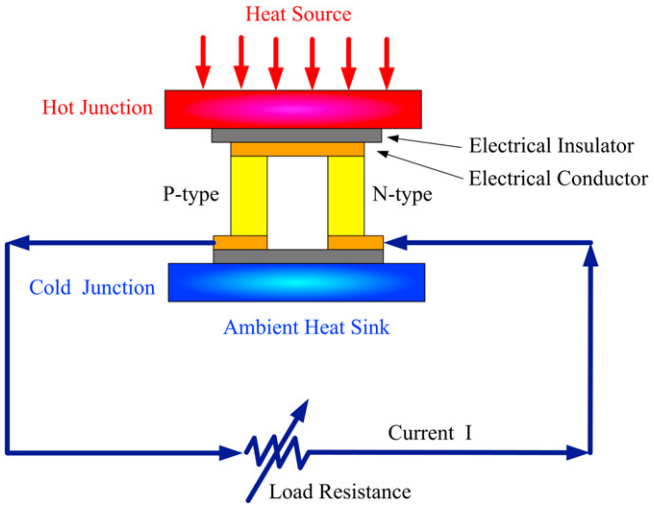

Fig. 1. Schematic of a working thermoelectric generator.

2. Experimental

2.1. Basics of TEG

The working principles of TEG include Seebeck effect, conduction effect and Joule effect. Seebeck effect explains the phenomenon that electric current induced by temperature difference in an electrical conductor, which simply describes the main function of a TEG. Typically, a commercial TEG is composed of ceramic substrates, electrical insulators, electrical conductors, and N-type/P-type semiconductor block. By applying different temperature on both sides of it, electric current is induced because of the thermoelectric effect. Fig. 1 shows the schematic of a working TEG.

In Fig. 1, the rates of supply heat (Q_H) and removal heat (Q_C) can be calculated at the hot and cold junction respectively.

$$Q_H = \alpha I \overline{T}_H + K(\overline{T}_H - \overline{T}_L) - \frac{1}{2} I^2 R_G \quad (1)$$

$$Q_C = \alpha I \overline{T}_L + K(\overline{T}_H - \overline{T}_L) + \frac{1}{2} I^2 R_G \quad (2)$$

2.2. TEG performance tests

Two different brands of commercial TEGs, H-type and T-type, were adopted for the performance tests. Table 1 shows their geometry characteristics. The heat source to the hot side and the cooling method for the cold side will influence the performance. A specific temperature difference on TEG is required to maintain a better outcome. Hence, a heater was used to provide continual energy to the hot side, and a micro channel heat sink was attached to the cold side to take the heat energy away. Water, as a coolant, circulated between the heat sink and a low temperature circulator bath. Fig. 2 presents the structure of experimental setup.

The heater was placed into a hollow Teflon block to prevent the heat loss from the ambient. The block enclosed the heater except the upper heating surface. 10 Thermocouples were installed on the block to measure the temperatures. By collecting the data of temperature differences between the inside and outside positions of block, the heat loss can be determined by Fourier's Law of Heat Conduction. The total heat loss (Q_l) consists of four side losses (Q_s) and one base loss (Q_b).

Table 1
Geometry characteristics of TEG.

Model	Length (mm)	Width (mm)	High (mm)	Weight (g)
HZ-2	29	29	5.08	13.5
TGM-127	40	40	3.9	32

$$Q_l = Q_s + Q_b \quad (3)$$

$$Q_s = 4k_T A_s \frac{T_{i,s} - T_{o,s}}{L_s} \quad (4)$$

$$Q_b = k_T A_b \frac{T_{i,b} - T_{o,b}}{L_b} \quad (5)$$

2.3. Performance coefficients of TEG

The performance of TEG can be characterized with Seebeck coefficient (α), internal electrical resistance (R_G) and thermal conductance (K).

The power generated from a TEG can be measured either by multiplying its output current with voltage, or observing the variation of heat flux.

$$P_o = V_o I_o = Q_H - Q_C \quad (6)$$

Subtract equation (2) from equation (1)

$$P_o = \alpha I(\overline{T}_H - \overline{T}_L) - I^2 R_G \quad (7)$$

the voltage can be expressed as

$$V_o = \frac{P_o}{I_o} = \alpha(\overline{T}_H - \overline{T}_L) - IR_G \quad (8)$$

when the power generation occurs at the condition of open circuit ($I = 0$), equation (8) becomes

$$V_o = \alpha(\overline{T}_H - \overline{T}_L) \quad (9)$$

The Seebeck coefficient (α) can be derived

$$\alpha = \frac{V_o}{(\overline{T}_H - \overline{T}_L)} \quad (10)$$

Apply equation (10) to equation (8) to obtain the value of internal electrical resistance (R_G). Consequently, substitute α and R_G into equation (1) to derive the value of thermal conductance (K). Take the first order partial derivatives of equation (7) with respect to I. By assuming the result on the left hand side of equation is zero [13], the output current I_o becomes

$$I_o = \frac{\alpha(\overline{T}_H - \overline{T}_L)}{2R_G} \quad (11)$$

The thermal efficiency of TEG can be calculated by

$$\eta_G = \frac{P_o}{Q_H} \quad (12)$$

2.4. Heat flux analysis of the TE module

TEGs with a heat exchanger system were designed to recover the waste heat from two positions, e.g. exhaust pipe and radiator on an automobile. To better understand the behaviors of each component in the module, a mathematic model was built to analyze the change of heat flux and predict the performance of system.

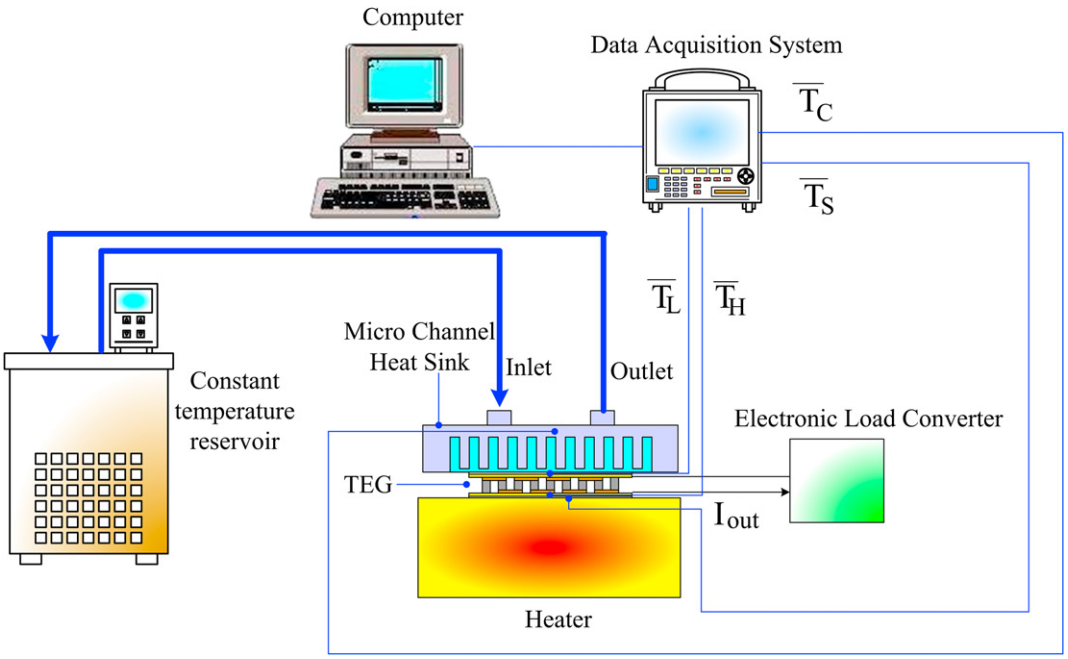

Fig. 2. The integral system for TEG performance test.

2.4.1. Thermal resistance model of the waste heat recovered from exhaust pipe

Fig. 3 illustrates a thermal resistance model, which recovers waste heat from the exhaust pipe. This model can be classified into three sections, the hot side, the cold side and TEG itself. The surrounding fluid of the hot side is exhaust gas and the cold side is the ambient air. The heat energy of exhaust gas depends on its temperature, however, the temperature increases with the engine speed.

Thermal resistance of hot side is composed of interface thermal resistance (R_i), material thermal resistance (R_m) and convectional thermal resistance (R_{conv}). The thermal resistance of cold side is composed of interface thermal resistance (R_i), spreading thermal resistance (R_{sp}), material thermal resistance (R_m) and convectional thermal resistance (R_{conv}).

When two materials contact with each other, thermal resistance occurs at the interface. It can be expressed as

$$R_i = \frac{t_i}{k_i A_c} \tag{13}$$

There is spreading thermal resistance when heat flows from a small area to a bigger area [14]

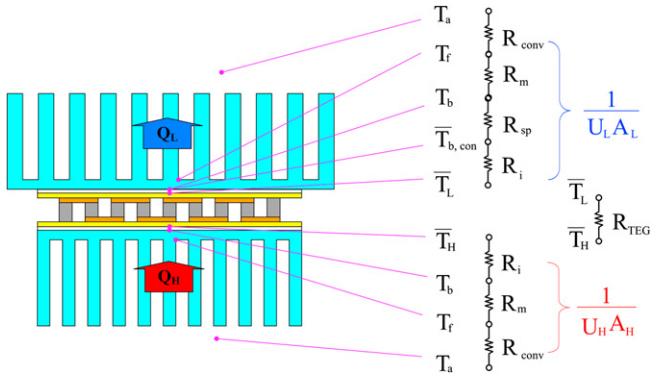

Fig. 3. One dimension thermal resistance model of the exhaust waste heat recovery module.

$$R_{sp} = \frac{\overline{T}_{b,con} - \overline{T}_b}{Q_C} - \frac{T_b - \overline{T}_b}{Q_C} = R_{sp,2} - R_{sp,1} \tag{14}$$

where

$$R_{sp,1} = \frac{\sqrt{A_b} - \sqrt{A_G}}{k_b \sqrt{\pi A_b A_G}} \times \Omega \tag{15}$$

$$\Omega = \frac{\lambda k_b A_b R_{conv} + \tanh(\lambda t_b)}{1 + \lambda k_b A_b R_{conv} \tanh(\lambda t_b)} \tag{16}$$

and

$$R_{sp,2} = \frac{1}{2k_b \sqrt{A_G}} \left(1 - \sqrt{\frac{A_G}{A_b}}\right)^{3/2} \times \Psi \tag{17}$$

$$\Psi = \frac{\lambda k_b A_b R_{conv} + \tanh(\lambda t_b)}{1 + \lambda k_b A_b R_{conv} \tanh(\lambda t_b)} \tag{18}$$

λ can be derived by

$$\lambda = \frac{\pi^{3/2}}{\sqrt{A_b}} + \frac{1}{\sqrt{A_G}} \tag{19}$$

The material thermal resistance at the base of heat sink is

$$R_m = \frac{t_b}{k_b A_b} = \frac{t_b}{k_b (W_b L_b)} \tag{20}$$

When there is a temperature difference between the fluid and solid surface, according to the Newton's Law of cooling, a convectional thermal resistance needs to be applied. It can be expressed as

$$R_{conv} = \frac{1}{h A_{eff}} \tag{21}$$

where the heat transfer coefficient h, according to [15], can be expressed as

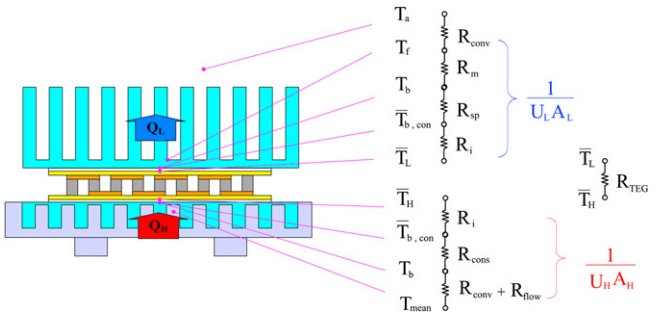

Fig. 4. One dimension thermal resistance model of the radiator waste heat recovery module.

$$h = \frac{0.037\mathrm{Re}^{4/5}\mathrm{Pr}^{1/3}}{H_f} \tag{22}$$

and the effective area is

$$A_{\mathrm{eff}} = \eta_f \times \left(2NWH_f\right) + (N-1)bW \tag{23}$$

where

$$\eta_f = \frac{\tanh\left(mH_f\right)}{mH_f} \tag{24}$$

$$m = \sqrt{\frac{hp}{k_f t_f}} = \sqrt{\frac{h \times \left[2 \times \left(t_f + L\right)\right]}{k_f \cdot \left(t_f \times L\right)}} \cong \sqrt{\frac{2h}{k_f \cdot t_f}} \tag{25}$$

Thermal resistance of TEG itself can be expressed as

$$R_{\mathrm{TEG}} = \frac{\overline{T}_H - \overline{T}_L}{Q_H - Q_C} \tag{26}$$

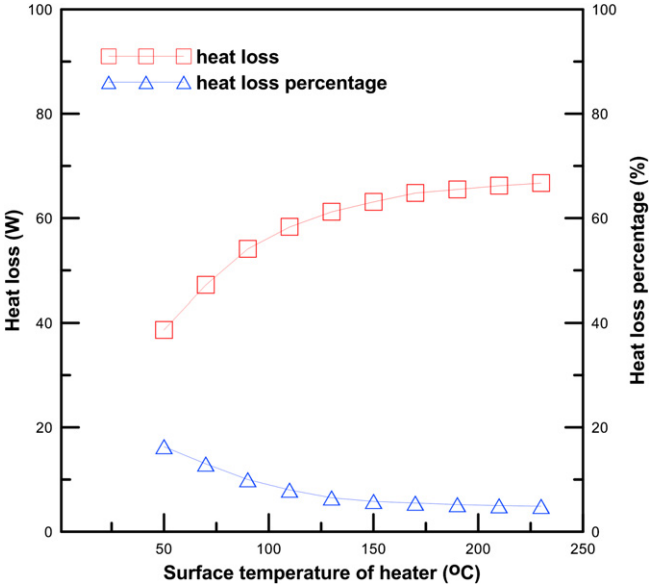

Fig. 5. The amount and percentage of heat loss from the heater at different surface temperature.

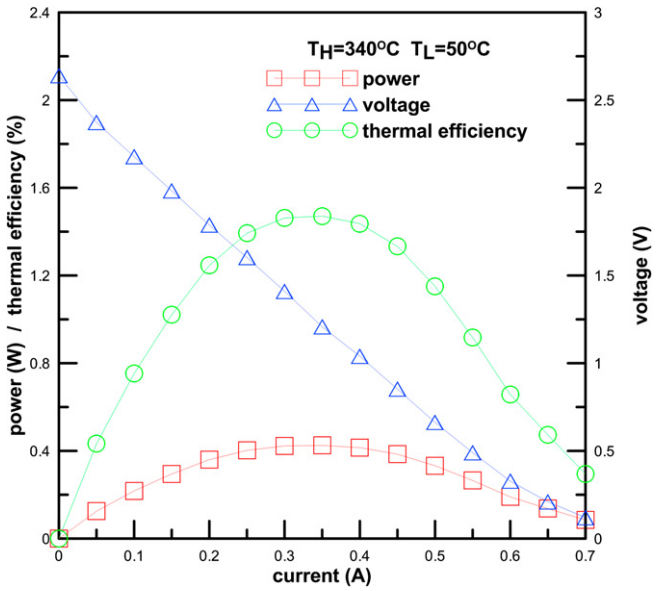

Fig. 6. The performance of H-type TEG at circumstance of $\overline{T}_H$ = 340 °C and $\overline{T}_L$ = 50 °C.

2.4.2. Thermal resistance model of the waste heat recovered from a radiator

Fig. 4 illustrates a thermal resistance model using TEG to recover waste heat from a radiator. This model consists of the hot side, the cold side and TEGs itself. The surrounding fluid in the hot side is the coolant (water) of radiator, and air is in the cold side. The coolant temperature increases with the engine speed. A micro channel heat sink is used to simulate the function of a radiator. The thermal resistance of the hot side is composed of interface thermal resistance, constriction thermal resistance, convectional thermal resistance and flow-rate thermal resistance. The thermal resistance of the cold side is the same with the previous model.

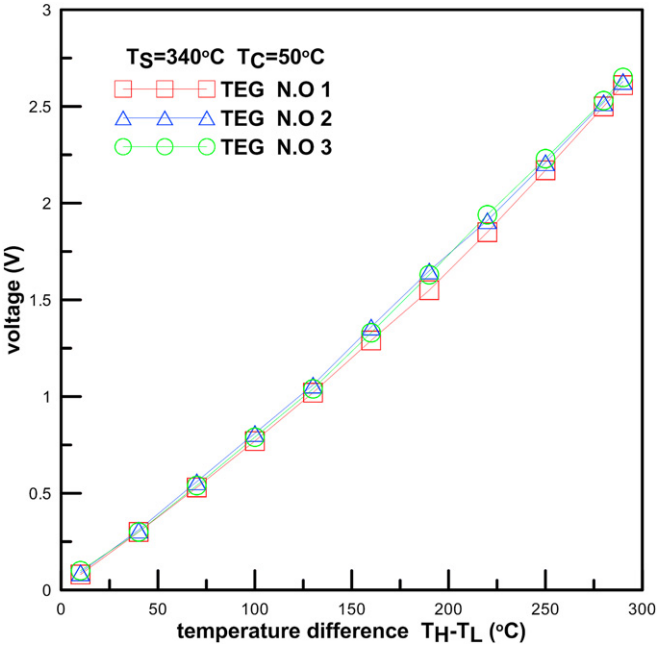

Fig. 7. The variation of output voltage with temperature difference on TEG.

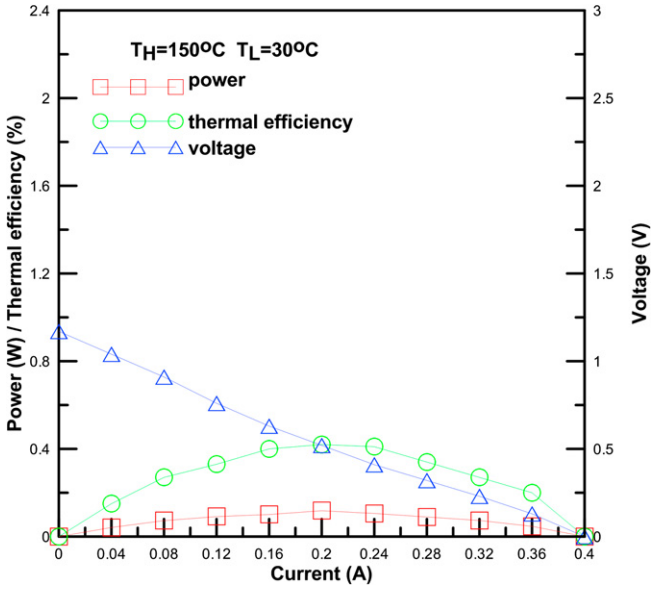

Fig. 8. The performance curves of T-type TEG at circumstance of $\overline{T}_H$ = 150 °C and $\overline{T}_L$ = 30 °C.

When the heat energy moves from a bigger area to a smaller area, there is a constriction thermal resistance [16]. It can be expressed as

$$R_{cons} = \frac{\varepsilon\tau + 0.5\sqrt{\pi}(1-\varepsilon)^{3/2}\Theta}{k_b \pi a} \tag{27}$$

where

$$\Theta = \frac{\tanh(\lambda\tau) + \lambda/Bi}{1 + \left(\lambda/Bi\right)\tanh(\lambda\tau)} \tag{28}$$

$$\lambda = \pi + \frac{1}{\varepsilon\sqrt{\pi}} \tag{29}$$

$$\mathrm{Bi} = \frac{1}{\pi k_b b\left(R_{conv} + R_{fl}\right)} \tag{30}$$

$$a = \sqrt{\frac{A_G}{\pi}} \tag{31}$$

$$b = \sqrt{\frac{W_{h,b}L_{h,b}}{\pi}} \tag{32}$$

$$\varepsilon = \frac{a}{b} = \sqrt{\frac{A_G}{W_{h,b}L_{h,b}}} \tag{33}$$

$$\tau = \frac{t_b}{b} \tag{34}$$

Table 2
Cost evaluations of H-type TEG.

HZ-2 output power	$\overline{T}_H = 300°C$, $\overline{T}_L = 10°C$	$\overline{T}_H = 320°C$, $\overline{T}_L = 30°C$	$\overline{T}_H = 340°C$, $\overline{T}_L = 50°C$
Maximum power (W)	0.35	0.40	0.43
Power per unit area (W/m^2)	416.2	475.6	511.3
Cost per unit power (USD/W)	173.8	152.1	141.5

Table 3
Cost evaluations of T-type TEG.

TGM-127 output power	$\overline{T}_H = 90°C$, $\overline{T}_L = 30°C$	$\overline{T}_H = 120°C$, $\overline{T}_L = 30°C$	$\overline{T}_H = 150°C$, $\overline{T}_L = 30°C$
Maximum power (W)	0.05	0.08	0.12
Power per unit area (W/m^2)	31.3	50.0	75.0
Cost per unit power (USD/W)	920.6	575.3	383.6

When the cooling water flows through the micro channel heat sink, the convectional thermal resistance at the interface of water and walls of heat sink is

$$R_{w,conv} = \frac{1}{hA} = \frac{1}{h_{eq}(W_{h,b}L_{h,b})} \tag{35}$$

According to [17], when the heat flow from the base of heat sink to the bulk fluid, the equivalent heat transfer coefficient can be expressed as

$$h_{eq} = \frac{h_m\left[2N\eta_f H_f + W_{h,b} - (N-1)t_f\right]}{W_{h,b}} \tag{36}$$

$$h_m = \frac{\mathrm{Nu}_m k_f}{D_h} \tag{37}$$

$$D_h = \frac{2W_{ch}H_f}{\left(W_{ch} + H_f\right)} \tag{38}$$

The mean Nusselt number, by the discussion of Copeland [18], can be expressed as

$$\mathrm{Nu}_m = \left\{\left[2.22\left(\frac{\mathrm{RePr}D_h}{L_{h,b}}\right)^{0.33}\right]^3 + \Pi\right\}^{1/3} \tag{39}$$

$$\Pi = (8.31G - 0.02)^3 \tag{40}$$

$$G = \frac{Ar^2 + 1}{(Ar+1)^2} \tag{41}$$

$$\mathrm{Ar} = \frac{W_{ch}}{H_f} \tag{42}$$

When the coolant flows through the heat sink channels, its inlet temperature will be different with the outlet temperature, hence the flow-rate thermal resistance needs to be considered. The heat transfer rate is

Table 4
Performance coefficients α, R_G and K of the H-type TEG.

HZ-2 Performance coefficient	α(V/°C)	$R_G(\Omega)$		K(W/K)
$\overline{T}_H = 300°C$ $\overline{T}_L = 10°C$	0.007	0.05A	3.77	0.097
		0.35A	3.23	
		0.70A	2.92	
$\overline{T}_H = 320°C$ $\overline{T}_L = 30°C$	0.008	0.05A	5.05	0.097
		0.35A	3.71	
		0.70A	3.36.	
$\overline{T}_H = 340°C$ $\overline{T}_L = 50°C$	0.009	0.05A	5.33	0.096
		0.35A	4.09	
		0.70A	3.60	
Average	0.008		3.89	0.097

Table 5
Performance coefficients α, R_G and K of the T-type TEG.

TGM-127 Performance coefficient	α(V/°C)	R_G(Ω)		K(W/K)
$\overline{T}_H = 90°C$ $\overline{T}_L = 30°C$	0.011	0.05A	2.00	0.464
		0.35A	1.88	
		0.70A	2.24	
$\overline{T}_H = 120°C$ $\overline{T}_L = 30°C$	0.010	0.05A	2.37	0.309
		0.35A	2.62	
		0.70A	3.36.	
$\overline{T}_H = 150°C$ $\overline{T}_L = 30°C$	0.010	0.05A	3.75	0.231
		0.35A	2.90	
		0.70A	2.97	
Average	0.010		2.62	0.334

$$\dot{Q} = \dot{m}\cdot C_p(T_o - T_{in}) = \frac{T_o - T_{in}}{1/\dot{m}\cdot C_p} \tag{43}$$

In order to define the properties of coolant inside the heat sink, mean temperature is adopted

$$T_{mean} = \frac{T_{in} + T_o}{2} \tag{44}$$

The flow-rate thermal resistance is

$$R_{fl} = \frac{1}{2\cdot\dot{m}\cdot C_p} = \frac{1}{2\cdot\left(\rho\cdot\dot{V}_f\right)\cdot C_p} \tag{45}$$

2.4.3. Operation parameters of TEG

In order to predict the output behaviors of a TEG, the overall thermal resistance and the overall heat transfer coefficient need to be known.

$$U_H = \frac{1}{R_{overall,H}\,A_H} \tag{46}$$

$$U_C = \frac{1}{R_{overall,L}\,A_L} \tag{47}$$

The rates of supply heat (Q_H) and removal heat (Q_C) can be expressed as

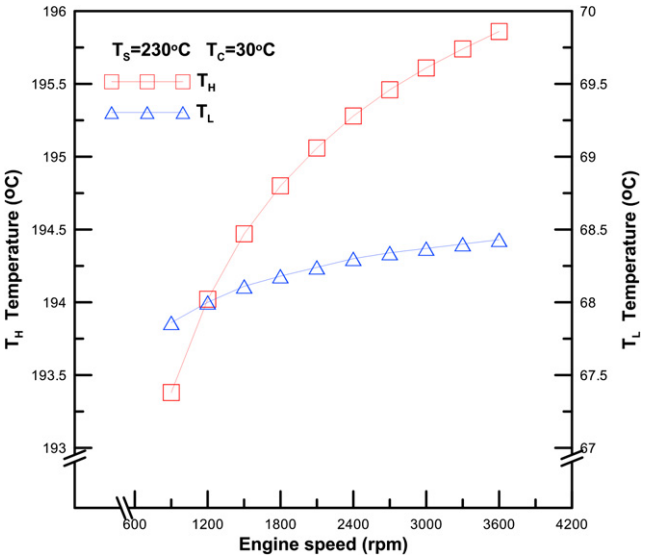

Fig. 9. The variation of temperatures ($\overline{T}_H$ and $\overline{T}_L$) with engine speed.

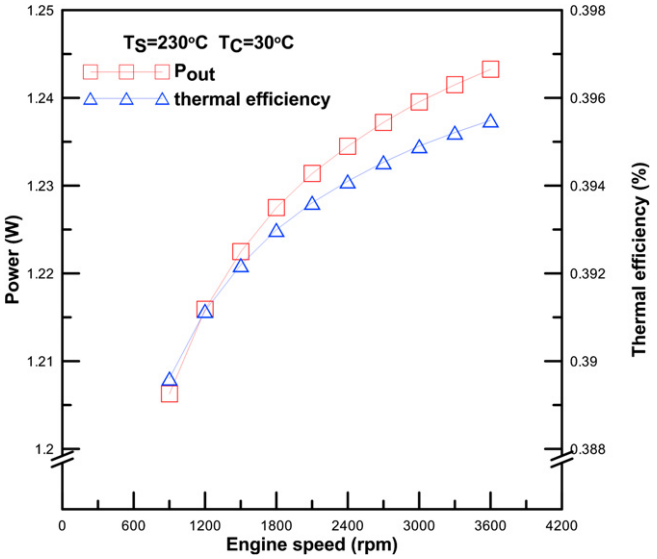

Fig. 10. The variation of simulated output power and thermal efficiency with engine speed.

$$Q_H = U_H A_H(T_S - \overline{T}_H) \tag{48}$$

$$Q_C = U_L A_L(\overline{T}_L - T_C) \tag{49}$$

Equate equation (1) with equation (48) and equation (2) with equation (49), the hot junction temperature ($\overline{T}_H$) and the cold junction temperature ($\overline{T}_L$) can be obtained by

$$\overline{T}_H = \frac{U_H A_H T_S + K\overline{T}_L + \frac{1}{2}I^2 R_G}{\alpha I + K + U_H A_H} \tag{50}$$

$$\overline{T}_L = \frac{U_C A_L T_C + K\overline{T}_H + \frac{1}{2}I^2 R_G}{U_C A_L + K - \alpha I} \tag{51}$$

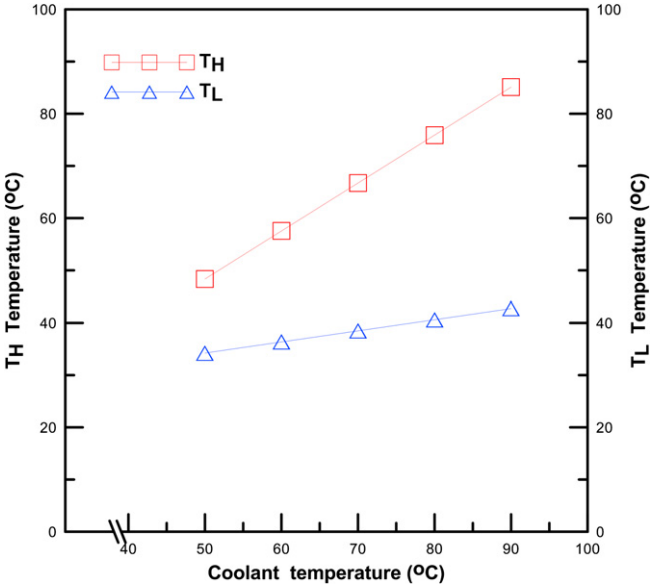

Fig. 11. The simulated results of two temperatures ($\overline{T}_H$, $\overline{T}_L$) related to the coolant temperature.

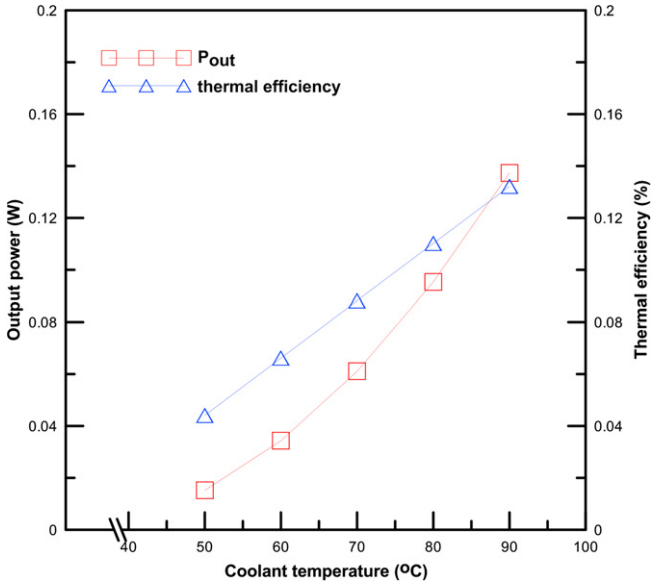

Fig. 12. Performance of an H-type TEG at different coolant temperature.

The values of $\overline{T}_H$ and $\overline{T}_L$ are derived by the iterative method. Substitute $\overline{T}_H$, $\overline{T}_L$, α and R_G into equation (11) to derive I_o. Replace $\overline{T}_H$, $\overline{T}_L$, α, R_G, k and I_o into equation (1), (2), (7) and (8) to find out the values of Q_H, Q_C, P_{out} and V_{out}.

3. Results and discussion

3.1. Analysis of the heat loss

To analyze the performance of a TEG, it is necessary to know the amount of heat delivered from the heater. Since the produced power is known from the specification provided by the vendor, the energy loss during the delivery from heater to TEG has to be measured first. Fig. 5 shows the amount of heat loss and the heat loss percentage at different heating surface temperatures. Experiment results indicate that the heat loss increases with the temperature of heating surface, but the percentage of heat loss reacts in the opposite way. The maximum heat loss is 66.7 W at 230 °C and the minimum is 38.6 W at 50 °C. The maximum heat loss percentage is 16.3% and the minimum is 4.9%. To have a more precise prediction, the heat loss is necessary to be considered in the model.

3.2. Performance curve and coefficients of a TEG

Two different TEGs, H-type and T-type, were tested as baseline data. Fig. 6 presents the variation of performance for an H-type TEG with current. The output voltage decreases with the increase of output current. At the current of 0.35 A, H-type TEG produces the maximum power of 0.43 W and reaches the highest thermal efficiency of 1.48%. Fig. 7 shows the relationship between voltage and temperature difference on both sides. The voltage variations are small at any temperature between 3 different test samples.

Fig. 8 presents the test results of a T-type TEG related to output current, the poor performance can be ascribed to the working environment. The required hot side temperature of H-type is higher than the T-type. Besides, H-type TEG can tolerate larger temperature difference and hence generate a higher output power. Tables 2 and 3 show the cost evaluations of two TEGs. The costs of TEGs were adopted with local dealers' prices in Taiwan. Tables 4 and 5 present the values of performance coefficient α, R and k under different working circumstances. Since the performance disparity, H-type TEGs were chosen for further experiments hereafter.

3.3. Modeling results of the module recovered waste heat from exhaust pipe

Fig. 9 illustrates the calculated results of $\overline{T}_H$ and $\overline{T}_L$ at different engine speeds. The temperatures of TEG at hot and cold junctions both increase with the increasing of engine speed. $\overline{T}_H$ depends on the temperature of exhaust gas, hence it is also related to the engine speed. The forced convection on the cold side will be improved by increasing the engine speed. However, the thickness of TEG is only 5.08 mm, when the heat spread from the hot junction to the cold junction, the cold side temperature is affected by the effect of heat conduction from the hot side. Therefore, the temperature increment in the hot junction will be higher than in the cold junction, the temperature difference of TEG still increases with the engine speed. The maximum temperature difference from simulation is 127.4 °C at 3600 rpm engine speed.

Fig. 10 shows the performance of a TEG at different engine speeds. Because the temperature difference increases with the engine speed, both output voltage and current become higher. Therefore, the output power and thermal efficiency of TEG are improved too. According to the mathematic model, the maximum values of output power and thermal efficiency are 1.24 W and 0.396% respectively at 3600 rpm engine speed.

3.4. Modeling results of the module recovering waste heat from radiator

Fig. 11 illustrates the calculated results of $\overline{T}_H$ and $\overline{T}_L$ of a TEG at different coolant temperatures. The results show that, the temperatures on both sides of TEG increase with the coolant temperature. From the model, the maximum temperature difference is 42.3 °C at the coolant temperature of 90 °C.

Fig. 12 shows the calculated output power and thermal efficiency of a TEG at different coolant temperatures. The output power increases as the coolant temperature increases. The maximum output power and thermal efficiency is 0.135 W and 0.135% respectively at coolant temperature of 90 °C.

4. Conclusion

This research has established fundamental analyses of TE modules applied on an automobile. The one TEG module can be extended to a TEG array to produce more electricity. It is practical to apply TEGs on an automobile to recover waste heat. The simulation results of mathematic model have been verified with experimental data and showing the consistence. The characteristic coefficients of a TEG were derived from a basic TEG performance test. Under designed working condition, a maximum power of 0.43 W was generated at 0.35 A current, and the maximum power density was 51.13 $mWcm^{-2}$.

In the simulation models of applications on an automobile, the temperature difference between the hot and cold junctions of TEG increased as the engine speed or the coolant temperature increase. The output voltage, according to the Seebeck effect, also increased as the temperature difference increase. Therefore, the output power and thermal efficiency can be improved. The temperature of cooling water is much lower than the exhaust gas, which caused a smaller hot temperature on the TEG hence induced a poor performance. Different materials suitable for lower temperature operation are needed for the radiator module.

Acknowledgements

The funds for this project were provided by the Hua-Chuang Automobile Information Technical Center Co., Ltd. The Authors are grateful to Prof. Jing-T Kuo, who has already retired from National Taiwan University, for his support and discussions.

Nomenclature

A	area (m^2)
b	tunnel width (m)
C	cooling source
C_p	specific heat at constant Pressure ($J\,Kg^{-1}$-K^{-1})
D	diameter (m)
H	high (m)
h	heat transfer coefficient ($Wm^{-2\circ}C^{-1}$)
I	output current (A)
K	thermal conductance (WK^{-1})
k	thermal conductivity ($Wm^{-1\circ}C^{-1}$)
L	length (m)
N	tunnel number
P	output power (W)
p	perimeter (m)
$\dot{Q}$	heat transfer rate (W)
Q_H	hot side heat transfer rate (W)
Q_C	cold side heat transfer rate (W)
R_G	internal electrical resistance of TEG (Ω)
R	thermal resistance (KW^{-1})
S	heat source
T	temperature (°C)
t	thickness (m)
U	overall heat transfer coefficient ($Wm^{-2\circ}C^{-1}$)
V	voltage (V)
W	width (m)

Dimensionless number

Bi	Biot number $\mathrm{Bi} = \dfrac{1}{\pi k_b b(R_{conv} + R_{fl})}$
Nu	Nusselt number $\mathrm{Nu} = h \cdot L / k_{fluid}$
Pr	Prandtl number $\mathrm{Pr} = \mu \cdot C_p / k$
Re	Reynolds number $\mathrm{Re} = VH_f / \nu$

Greek symbols

α	Seebeck coefficient ($V^{\circ}C^{-1}$)
μ	dynamic viscosity ($N \cdot S \cdot m^{-2}$)
ν	kinematic viscosity ($m^2 \cdot s^{-1}$)
η	efficiency (%)

Subscripts

b,con	base mean temperature
b	base of Teflon block
C	cooling fluid temperature
c	contact surface
ch	channel
conv	convection
cons	constriction
eq	equivalent
eff	effective area
f	fin
fl	flow rate
G	TEG
h	hydraulic
h,b	heat sink base
H	hot side
i	interface
i,b	inner base of Teflon block
i,s	inner side of Teflon block
L	cold side
l	heat loss
m	material
o	output
o,b	outer base of Teflon block
o,s	outer side of Teflon block
p	constant pressure
S	heat source temperature
s	side of Teflon block
sp	spreading
T	Teflon block
w, cv	convection between water and wall

References

[1] Birkholz U, Grob E, Stohrer U, Voss K. Conversion of waste exhaust heat in automobiles using FeSi2 thermoelements. Proceedings of the 7th International Conference on Thermoelectric Energy Conversion, Arlington, USA; 1988. pp. 124–128
[2] Bass JC, Campana RJ, Elsner NB, Thermoelectric generator for diesel engines. Proceedings of the 1990 Coatings for Advanced Heat Engines Workshop, U.S.,; 1990
[3] Bass JC, Campana RJ, Elsner NB. Thermoelectric generator for diesel trucks. Proceedings of the 10th International Conference on Thermoelectrics, Cardiff, Wales; 1991
[4] Bass JC, Elsner NB, Leavitt A. Performance of the 1 KW thermoelectric generator for diesel engines. Proceedings of the 13th International Conference on Thermoelectrics, New York; 1995
[5] Bass JC. Thermoelectric generator for motor vehicle. U.S. Patent US5625245, April 29; 1997
[6] Bass JC, Elsner NB, Leavitt FA. Method for fabricating a thermoelectric module with gapless eggcrate. U.S. Patent US 5856210, January 5; 1999
[7] Kobayashi M, Ikoma K, Furuya K, Shinohara K, Takao H, Miyoshi M, Imanishi Y, Watanabe T. Thermoelectric generation and related properties of conventional type module based on Si–Ge alloys. Proceedings of the 15th International Conference of Thermoelectric; 1998
[8] Ikoma K, Munkiyo M, Furuya K, Kobayashi M, Komatsu H, Shinohara K. Thermoelectric generator for gasoline engine using Bi_2Te_3 modules. J Japan Inst Met 1999;63(11):1475–8.
[9] Thacher E, Helenbrook B, Karri M, Richter C. Testing of an automobile exhaust thermoelectric generator in a light truck. Proc Inst Mech Eng Part D J Automob Eng 2007;221(1):95–107.
[10] Matsubara K. The performance of a segmented thermoelectric converter using Yb-based filled skutterudites and Bi2Te3-based materials. MRS 2001 Fall Proceedings, Symposium G, vol. 691; 2001, G9.1
[11] Matsubara K. Development of a high efficient thermoelectric stack for a waste exhaust heat recovery. Proceedings of ICT'02, 21st International Conference on thermoelectrics; 2002, pp. 418–423
[12] Champier D, Bedecarrats JP, Rivaletto M, Strub F. Thermoelectric power generation from biomass cook stoves. Energy, In Press, doi:10.1016/j.energy.2009.07.015
[13] Wu C. Analysis of waste-heat thermoelectric power generator. Appl Therm Eng 1996;16(1):63–9.
[14] Lee S, Song S, Au V, Moran KP. Constriction/spreading resistance model for electronic packing. ASME/JSME Thermal engineering Conference, 4; 1995. pp. 109–206
[15] Çengel YA. Heat transfer a practical approach. McGraw-Hill, ISBN 0-07-115223-7; 1998. pp. 177–192 & 350-363.
[16] Lee S. Optimum design and selection of heat sinks. IEEE Trans Compon Packag Manuf Technol Part A 1995;18(4):812–7.
[17] Kraus AD, Bar-Cohen A. Design and analysis of heat sinks. John Wiley & Sons, Inc, ISBN 978-0-471-01755-4; 1995.
[18] Copeland D. Optimization of parallel plate heat sinks for forced convection. Proceedings of 16th IEEE SEMI-THERM Symposium; 2000. pp. 266–272